Sedimenting discs in a two-dimensional foam

I. T. Davies, S. J. Cox

Institute of Mathematics and Physics, Aberystwyth University, Aberystwyth SY23 3BZ, UK

Abstract

The sedimentation of circular discs in a dry two-dimensional, monodisperse foam is studied. This, a variation of the classical Stokes experiment, provides a prototype experiment to study a foam's response. The interaction between two circular particles of equal size and weight is investigated as they fall through the foam under their own weight. Their positions are tracked and the lift and drag force measured in numerical calculations using the Surface Evolver. The initial placements of the discs are varied in each of two different initial configurations, one in which the discs are side by side and the second in which the discs are one above the other. It is shown that discs that are initially side by side rotate as a system during the descent in the foam. In the second scenario, the upper disc falls into the wake of the lower, after which the discs sediment as one with a constant non-zero separation. We present evidence that the foam screens this interaction for specific initial separations between the discs in both configurations. The force between a channel wall and a nearby sedimenting disc is also investigated.

Key words: Surface Evolver, discs, sedimentation, interaction
PACS:

1 Introduction

Liquid foams are familiar materials used domestically and in industrial processes such as ore-separation and enhanced oil recovery [1–3]. They are characterized as elasto-visco-plastic complex fluids due to their highly non-linear response to applied stresses. At low stresses they can be considered elastic solids, while increasing the applied stress results in plastic events. Plasticity in a foam is described by topological changes T_1s, where a neighbour-swapping of bubbles occurs in response to the applied stress. Increasing the applied stress above a foam's yield stress results in viscous liquid-like behaviour [4]. Thus, foams provide a prototype complex fluid with which it is possible to work at a macroscopic bubble scale instead of the usual molecular scale.

We use a variation of the classical Stokes' experiment [5], originally used to measure the viscosity of a fluid through which a sphere is dropped, to describe and understand these elasto-visco-plastic transitions in foam rheology.

Existing work on experiments in which a constant force is applied to a particle in a foam is limited to a single sphere [6]. Other work where foam flow is probed by a fixed sphere uses the variation in drag force on the particle to quantify the foam response [7,8]. This scenario has proved useful in describing foam aging [9,10].

Two-dimensional foams can be thought of as a monolayer of bubbles squeezed between two glass plates. We choose to probe the foam response by dropping circular obstacles of greater size than the bubbles into a foam channel. Existing work on smaller particles in foam concentrates on the dispersion of particles within the Plateau borders that constitute the liquid network of the foam [11,12]. Two-dimensional experiments using circular obstacles to probe foam response are a simplification of the 3D case but provide a clearer description. The drag force on a circular obstacle due to the foam has been measured through image analysis [13,14] and it was found to increase with obstacle size and decrease with bubble size while the roughness of the obstacle was not important. Confinement in two dimensions means that images of the foam during such experiments provide information on foam deformation fields as well as bubble velocity and pressure fields [15]. Combining such experiments with simulation has proved beneficial in showing that the drag force on a circular obstacle is also inversely correlated with the liquid fraction of the foam [16]. Combining the work of [13] and [16], the drag force on a circular obstacle of diameter d_0 is approximately $\phi^{-\frac{1}{4}} d_0/\sqrt{A_b}$ where A_b is the bubble area in a two dimensional foam and ϕ its effective liquid fraction.

Experiments investigating the flow of foam past different shaped obstacles, such as a cambered airfoil [17] and an ellipse [18], have enhanced the understanding of foam response. An inverse lift force was observed for the cambered airfoil when placed in foam flow while the ellipse rotated so that its axis was parallel with the foam flow for every initial placement. This is known to be a feature of elastic fluids [19]. Thus, we aim to answer the question of whether the plasticity of foam is significant in determining the way in which particles sediment within a foam, and can we therefore treat the foam as an elastic liquid? Moreover, does a foam screen the interaction between particles as it does for the effects of topological changes within its structure [20]?

We choose to work in two dimensions for the reasons stated. We use the Surface Evolver [21] to simulate the sedimentation and interaction of two circular discs falling under their own weight. We look at the position of the discs as

they descend and analyze the time-varying forces on them. The resultant force is split into two: the drag contribution parallel to the direction of gravity and the lift force perpendicular to gravity. We consider the low velocity limit, in which we expect that the dominant contributions to these forces come from the tensions of the soap films (network force) and the pressures of the bubbles (pressure force) – see figure 1. We aim to understand the conditions under which two objects falling through a foam are mutually attracted or repelled, as has been done for a number of purely viscoelastic fluids [22–25].

2 Method

An obstacle descends through a foam under the action of five forces: (i) its weight; (ii) the resultant tension force $\vec{F}^n$ due to the network of films pulling on it; (iii) the resultant pressure force $\vec{F}^p$ due to the pressure of bubbles contacting it; (iv) the viscous force $\vec{F}^\eta$ which opposes movement of the films around its circumference; and (v) the frictional force due to the interaction of its plane faces with the bounding surfaces, proportional to its velocity. Note that the films that are in contact with the obstacle are not uniformly distributed around the circumference – they bunch up behind the obstacle, as shown in figure 2 – so that the resultant network and pressure forces are usually non-zero.

Newton's second law applied to each disc of mass m gives

$$m\frac{d^2\vec{x}(t)}{dt^2} = mg\hat{y} - \lambda\frac{d\vec{x}(t)}{dt} + \vec{F}^p + \vec{F}^n + \vec{F}^\eta, \tag{1}$$

where $\vec{x}(t)$ denotes the position of the disc at time t, g is the acceleration due to gravity, and $\hat{y}$ is a unit vector pointing vertically downwards. λ is a friction coefficient due to the interaction of the plane faces of the discs with the bounding surfaces.

We simulate sedimentation in a dry 2D foam by tracking the motion of two discs commencing from a position near the top of a foam channel [26]. We assume that the motion is slow and steady, so that we may neglect the acceleration term and the viscous forces. The model simplifies to the following evolution equation, controlled by just three forces (see figure 1):

$$\frac{1}{\epsilon}\frac{d\vec{x}(t)}{dt} = mg\hat{y} + \vec{F}^p + \vec{F}^n, \tag{2}$$

where $\epsilon = 1/\lambda$ sets the effective time scale of the motion.

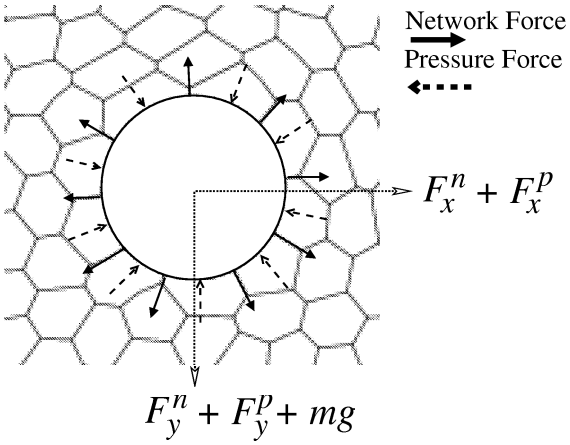

Fig. 1. The positions of the discs evolve under the gravitational, tension and pressure forces shown. Each force is resolved into its horizontal and vertical (the direction in which gravity acts) components.

For each disc the resultant network force is the sum of the tension force due to those films j that touch the disc. Since viscous drag around the disc is neglected, each film meets the disc perpendicularly [27] and makes an angle θ_j with the positive y direction. Thus

$$\vec{F}^n = \gamma \sum_{\text{films } j} (\sin\theta_j, \cos\theta_j) \tag{3}$$

where γ is the line tension of each film. The pressure force is a sum over all the bubbles k touching the obstacle

$$\vec{F}^p = \sum_{\text{bubbles } k} p_k l_k (\sin\theta_k, \cos\theta_k) \tag{4}$$

where p_k is the pressure inside the bubble, l_k is the length of the contact line of the bubble with the disc and θ_k is the angle that the inward normal at the midpoint of l_k makes with the positive $y-$direction.

The simulation proceeds from a Voronoi construction [29] which is used to generate a fully periodic tessellation of the plane. Bubbles at the left and right-hand sides of the structure are sequentially deleted until the required number remains. The structure is then imported into the Surface Evolver [21] and the peripheral films are constrained to one of the two side walls.

Using the Surface Evolver in a mode in which each film is represented as a circular arc, we perform quasi-static simulations. We use four different foams in a channel of length $L = 1$, with between $N = 727$ and $N = 2200$ bubbles.

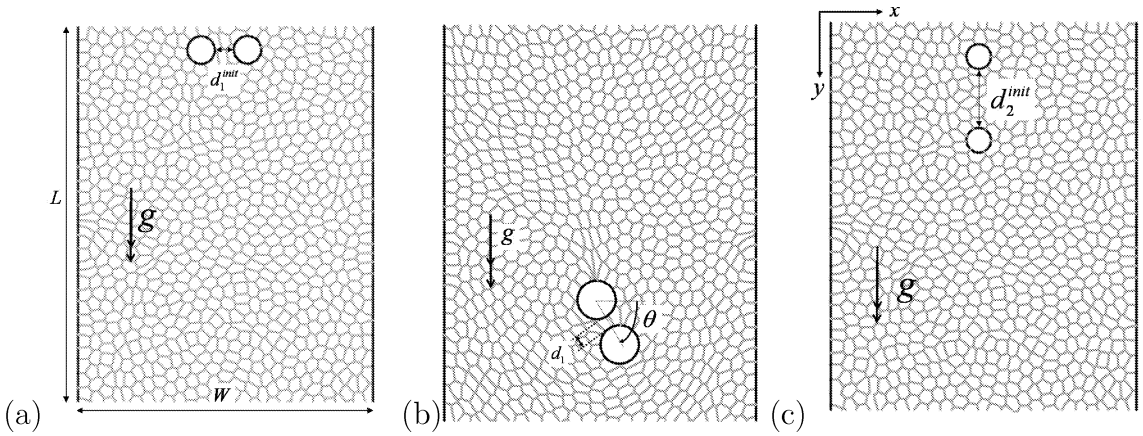

Fig. 2. Two discs sedimenting in a monodisperse foam contained in a channel of width W and length L. (a) Configuration 1, in which the discs start side by side, with a distance d_1^{init} between their centres. (b) If the discs rotate about one another we measure an angle θ between the positive $x-$direction and the line between the discs' centres. (c) Configuration 2, in which the discs start one above the other, a distance d_2^{init} apart.

The width of the channel decreases from $W = 0.8$ for the lowest N to $W = 0.4$ for $N = 2200$. We work with monodisperse foams, with the bubble area $A_b \approx LW/N$ (A_b shrinks slightly in proportion to the disc size, since the total area of the foam and two-disc system is constant). The cut-off length [27,16] for T_1 events is chosen to keep the liquid fraction $\phi < 0.1\%$, appropriate for a dry foam, giving l_c of the order of 10^{-3}. In all cases the channel is periodic in the $y-$direction, parallel to the direction of gravitational acceleration. The simulations are stopped before either of the discs return to the top of the foam channel. We set a no-slip condition at the channel wall: the foam films that touch the walls have fixed vertices. The films that are in contact with a disc are free to slip.

We choose dimensionless units such that the line tension γ has value 1 throughout. We keep the disc weight fixed throughout our simulations at $mg = 10$, and the areas of both discs are equal. It was ensured that this disc weight was sufficiently large that the discs were not brought to a halt by the foam, for all disc areas A_d considered.

The simulations proceed as follows: a foam containing the two discs in their starting positions is relaxed to equilibrium, using the method described in [26]. The resultant forces on the discs in the x and y directions are calculated and the disc centres moved according to

$$\begin{aligned} \Delta x &= \epsilon(F_x^n + F_x^p) \\ \Delta y &= \epsilon(F_y^n + F_y^p + mg) \end{aligned} \tag{5}$$

where the subscripts denote the x and y components of the forces. The parameter ϵ measures how far the centres move at each iteration (we used $\epsilon = 5\times10^{-4}$ for foams of less than 1000 bubbles, and $\epsilon = 2 \times 10^{-4}$ otherwise). The foam perimeter is then brought back to a local minimum with the discs fixed. This comprises one iteration, which is repeated until a disc reaches the bottom of the foam channel. The computational time is dependent upon the number of bubbles: the simulations take about 50 hours for the smallest foams and more than 120 hours for the largest.

We first examine the sedimentation of a single disc in the foam to quantify the wall effects and check that the rest of the simulations will be independent of such effects (Section 3.1). We then choose two main initial configurations for our two disc sedimentation simulation, as shown in figure 2. The disc centres are initially separated by a distance d_i^{init}, either horizontally $i = 1$ or vertically $i = 2$.

3 Results

3.1 Single disc falling near a vertical wall

We vary the initial placement of a single disc of area $A_d = 4A_b$ at the top of the channel so that the effects of the wall on the motion of the disc could be ascertained, in the hope of being able to neglect it when considering the interaction of two discs. We track the disc motion for nine different initial placements, the first being $0.1W$ away from the left wall in increments of $0.1W$, the last being $0.1W$ from the right wall. This is done for the small foams with $N = 727$ and 746.

It was found that for a fixed obstacle placed in a flow of foam in a similar channel the wall repels the obstacle [27], while sedimenting particles in viscoelastic fluids are attracted to walls [28]. Figure 3 demonstrates the drag ($-F_y^n - F_y^p$, acting in the vertical direction) and lift ($F_x^n + F_x^p$, acting in the horizontal direction) forces on a disc as it falls through the foam. There is an initial transient during which the forces rise; they then saturate but fluctuate greatly. The sudden drops in each force occur when a bubble detaches from the back of a disc. We therefore take average values for the forces after the transient, shown as horizontal lines.

Figure 4(a) demonstrates the variation in average drag force on a disc as it

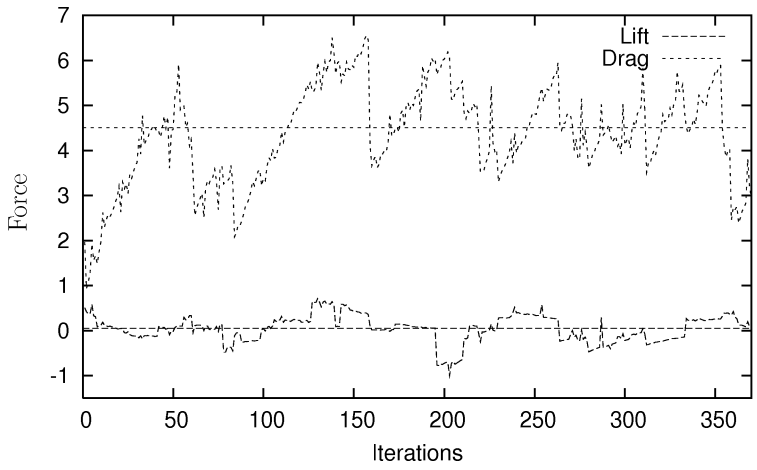

Fig. 3. The variation in drag and lift force on one disc (placed in the centre of the channel) as it descends through the foam. The plots are non-smooth due to the foam structure; jumps in the force appear when T_1s occur. Note that a transient occurs for roughly the first 100 iterations. We record the average and standard deviation of the drag and lift force after this transient.

falls from different positions at the top of the foam channel. We deduce that a disc's proximity to the walls does not have a large effect on the drag force exerted by the foam; there is only a slight decrease in drag. Figure 4(b) shows the average lift force on a disc as it descends through the foam. It can be seen that for discs that are released close to either of the walls, there is a small lift force that is in the direction of the nearest wall. For example, a negative lift on the left hand side of the plot demonstrates that the force is to the left and *vice versa*. These forces are considerably smaller and fluctuate less than the drag force. The attractive force between a disc and a nearby wall, although small, appears robust with respect to different foams.

3.2 Two discs in configuration 1

We investigate the interaction of two discs placed side by side close to the centre of the foam channel, where we can neglect wall effects, that is, in the region $0.3W < x < 0.7W$. The initial separation between the discs and the areas of the discs are varied and we investigate whether the discrete nature of the foam screens [20] the interaction between the discs. For each simulation, we record at each iteration the disc positions (figure 5) and the drag and lift forces on each one.

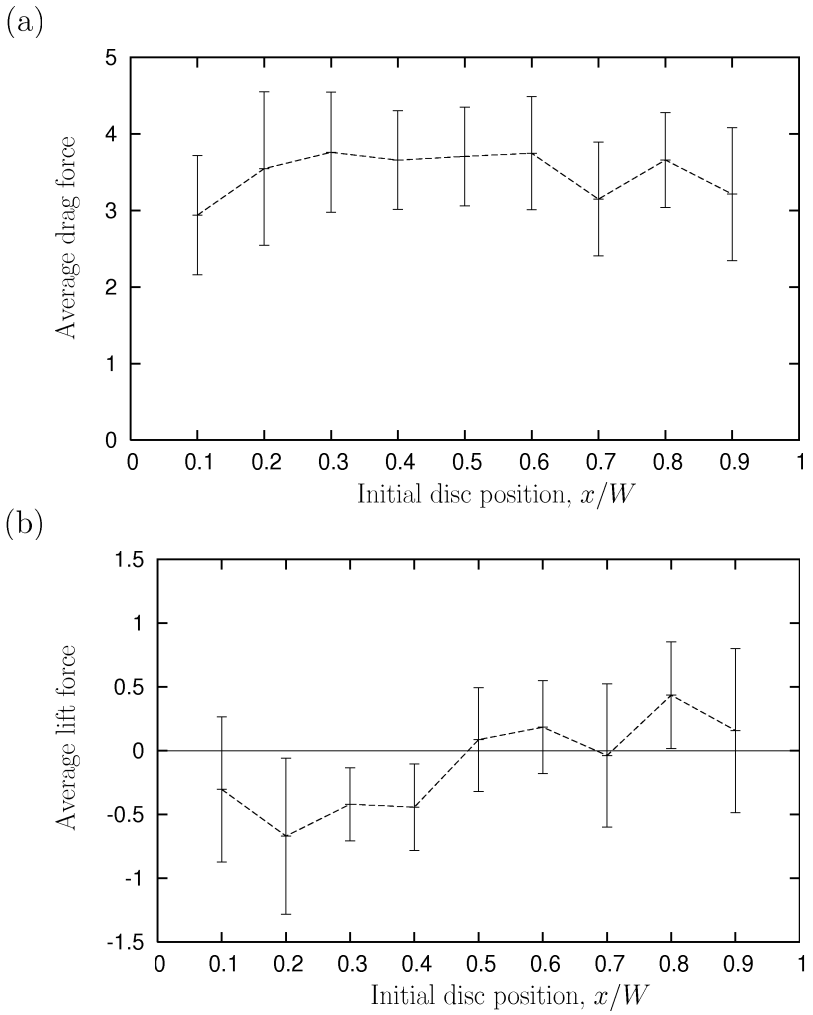

Fig. 4. (a) The variation of the average drag force on a disc as it descends through the foam from different positions along the top of the channel. The disc is placed in each of nine positions at equal intervals of $0.1W$. The average drag force on a disc decreases slightly close to the walls. Error bars indicate the standard deviation in force for each simulation, after the transient. (b) The variation of the average lift force on a disc for the same initial placements as (a). The positive direction of the force is to the right. Thus lift is negative when the disc falls from $0.1W$ (close to the left wall) and positive when falling from $0.9W$ (close to the right wall) therefore a small attractive force on the disc from the walls exists.

3.2.1 Disc Position

It has been shown that in a viscoelastic fluid circular particles in this configuration rotate about one another as they sediment [22–25]. We find the same rotation in foams: figure 6(a) shows the variation of the angle between two discs of area $4A_b$ as they descend. The rotation of the disc system can occur in either a clockwise or an anticlockwise manner. Thus the plasticity of the material doesn't change the sedimenting motion of the particles greatly.

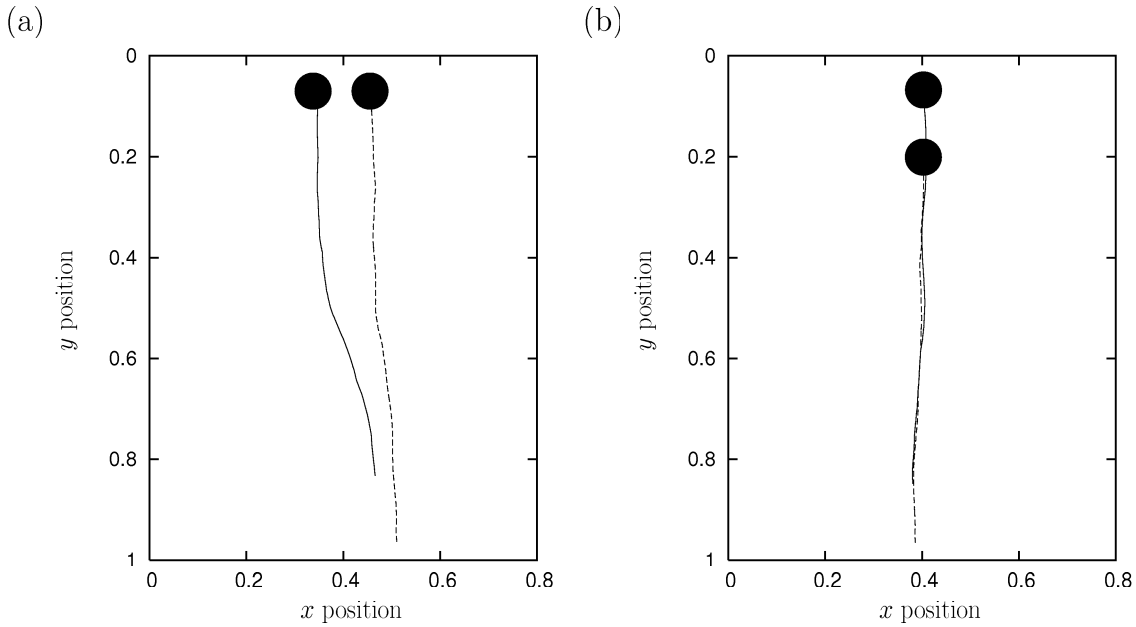

Fig. 5. Tracking the motion of the discs' centres in two typical simulations. Left: Configuration 1, with $d_1^{\text{init}} = 0.08$ and $A_d = 4A_b$. Here, both discs move a short distance to the right, and the disc initially on the left advances more slowly and moves behind the right-hand disc. Right: Configuration 2, with $d_2^{\text{init}} = 0.2$ and $A_d = 4A_b$. The discs barely deviate to the sides, but the upper disc moves slightly faster into the lower disc's wake.

In figure 6(a) it is apparent that discs that are initially close together rotate until they reach a plateau value at $|\theta| = \frac{\pi}{2}$. In this case the discs have rotated from configuration 1 to configuration 2. The plateau at $|\theta| = \frac{\pi}{2}$ demonstrates that once the discs are directly above one another, they stay in this configuration. Notice that there are some simulations which don't reach these plateau values: those in which θ doesn't change dramatically are the ones for which the discs were initially too far apart. Others are those in which the foam was too short for the plateau to be reached.

There is a strong relationship between the initial separation of the discs and the settling angle (the angle between the discs after reaching the bottom of the foam). Discs that are initially far apart rotate less. We look more closely at this trend by fitting the data for the settling angle (figure 6b) to the following model:

$$|\theta| = \frac{\pi}{4}\left(1 + \tanh\left(\kappa \frac{(d_1^c - d_1^{\text{init}})}{d_b}\right)\right), \tag{6}$$

where d_1^c is the critical initial separation above which the discs do not interact, d_b is the average bubble diameter and the slope is $\kappa = N/1000$ which measures the extent to which the plateau has been reached.

(a)

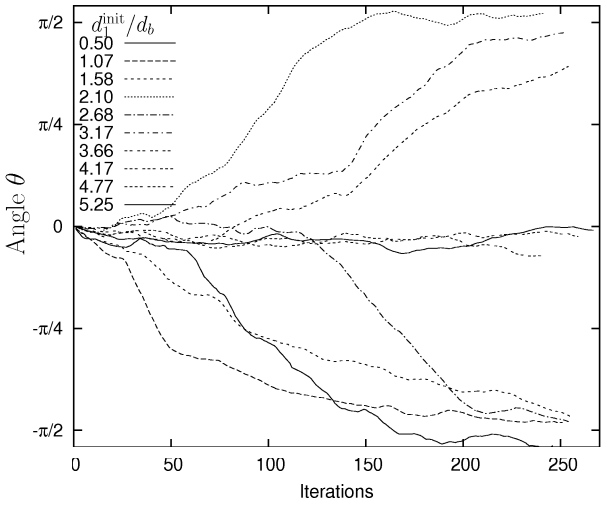

(b)

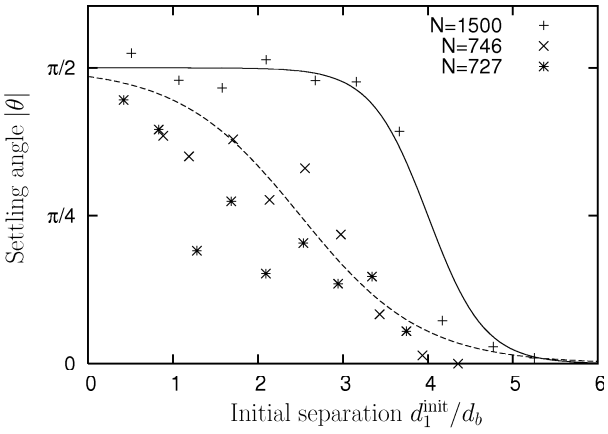

(c)

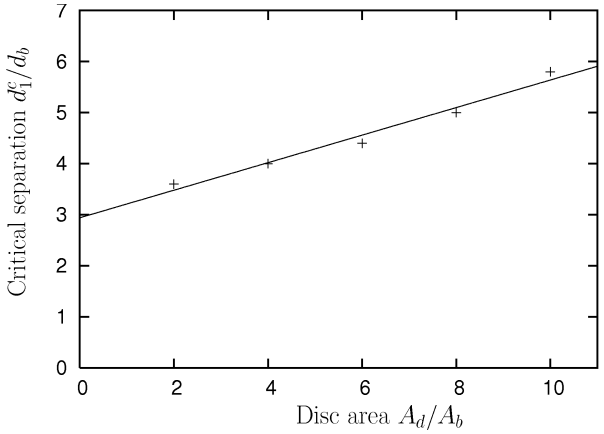

Fig. 6. (a) The angle θ between the disc centres in configuration 1 with $N = 1500$ bubbles and $A_d = 4A_b$ for a range of initial separations $d_1^{\rm init}$. θ increases in either a clockwise and anticlockwise direction, demonstrating rotation of the discs. If close enough, the discs rotate into configuration 2 and stay in this configuration. (b) The settling angle ($|\theta|$ at the bottom of the channel) of two discs with $A_d = 4A_b$ fitted to a tanh function, eq. (6). The foam screens the interaction of the discs if they are initially 4 or more bubble diameters apart. The lower slope for the smaller foams is due to the foam being too short for the full rotation to occur. (c) The critical separation below which the discs interact and rotate increases with disc size. The line is a linear fit.

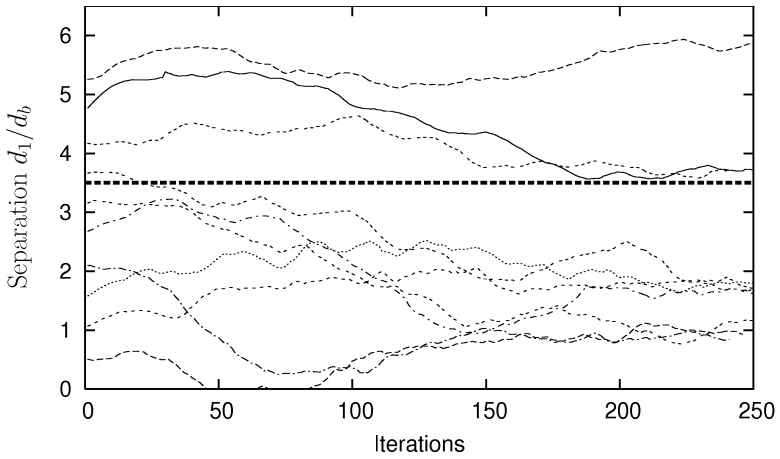

Fig. 7. The separation between disc edges, measured in bubble diameters, as they fall through a foam with $N = 1500$ bubbles in configuration 1. Disc area is $A_d = 4A_b$. If they are initially placed sufficiently close together, there is a tendency for the discs to move together so that they are separated by one to two bubbles. The horizontal dashed line represents a critical value above which the interaction between the discs is negligible.

We find $d_1^c = (4 \pm 1)d_b$ for discs of area $A_d = 4A_b$. Thus, if the discs initially have more than four bubbles in between them then they don't interact and rotate. When the discs are closer than this they will rotate until they reach configuration 2 in which they are one above the other. Figure 6(c) demonstrates the variation in the critical screening length for different disc size. The critical length d_1^c increases with disc size. Thus larger discs interact at a greater separation. We note also that larger discs rotate at a slower rate, so that a longer foam is required (we used $N = 2200$ bubbles).

The variation of disc separation is also important when looking at their motion. In figure 7 we see that this is highly dependent on their initial separation. For discs of area $A_d = 4A_b$ that are initially close ($0 < d_1^{\text{init}} < 4d_b$), there is a tendency for them to move together so that they are separated by $1 - 2d_b$. (There is one case here where the discs have moved so close together during sedimentation that they are touching, but they then separate and follow the same pattern.) Discs that are initially placed further apart than the critical separation don't move closer in the same manner. In some cases, the discs even move away from each other. We believe that for large separations any variation in separation arises from inhomogeneities in the foam structure, as there is no clear trend.

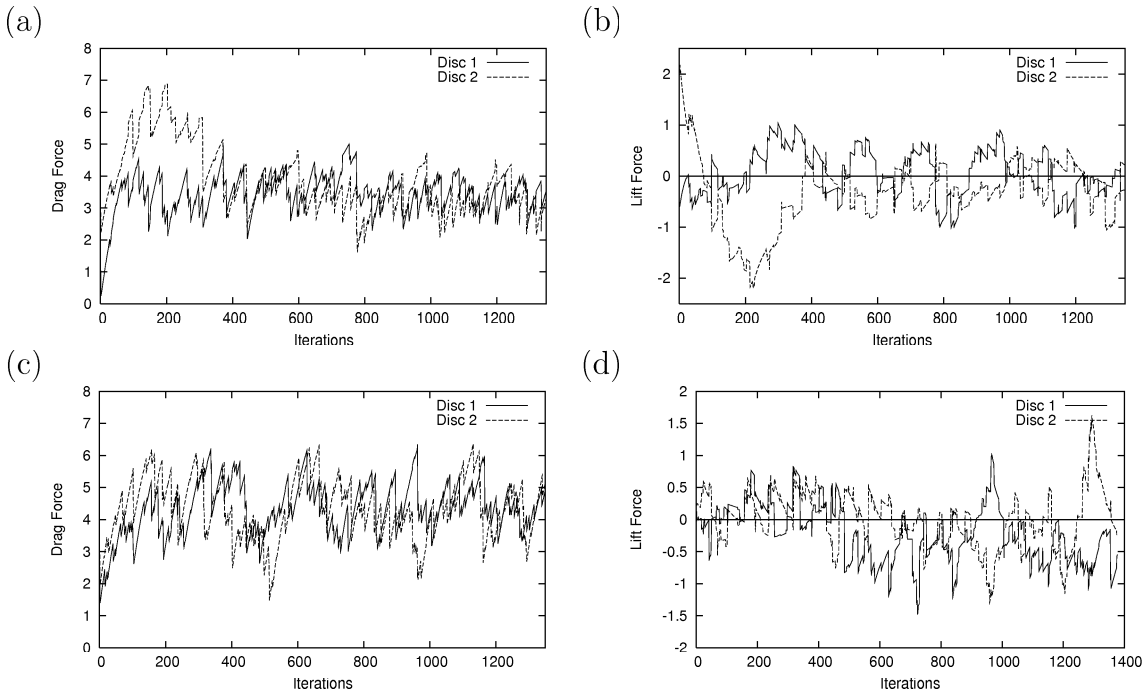

Fig. 8. Fluctuating forces on two discs in configuration 1. (a) drag force on both discs for ${d_1}^{\text{init}} = 0.64d_b$, (b) lift force on the discs when ${d_1}^{\text{init}} = 0.64d_b$. It can be seen that there is an overshoot in the drag for disc 1 in (a) and then an overshoot in the lift on disc 1 in (b). Thus, they interact and rotate about one another. (c) and (d) Same data for two discs that start further apart (${d_1}^{\text{init}} = 4.20d_b$). Here the drag and lift forces are very similar for both discs and follow the same pattern as would be expected on one disc falling in the foam. Thus, the discs don't interact in this case.

3.2.2 Forces on the Discs

We look at how the forces on the discs induce the interaction between the discs, considering only the case $A_d = 4A_b$. Figure 8 shows the drag and lift forces from two different simulations in the $N = 1500$ foam. The first is for two initially close discs that rotate and the second is for two discs that are too far apart to interact. When the discs are initially close together, the drag force is seen to overshoot for one of the discs. This results in slower downward motion of this disc and it is left trailing. An increase in the lift force is seen for this disc at this stage and it is directed so that the disc moves into the wake of the other disc. Thus, the discs begin to rotate so that the resistance to their downward descent is minimized. After rotation has occurred it can be seen that the drag and lift forces on both discs become very similar, at which point the motion of the discs becomes more stable. For the discs that were initially further apart no such overshoots are seen as they don't interact (figure 8(c) and (d)).

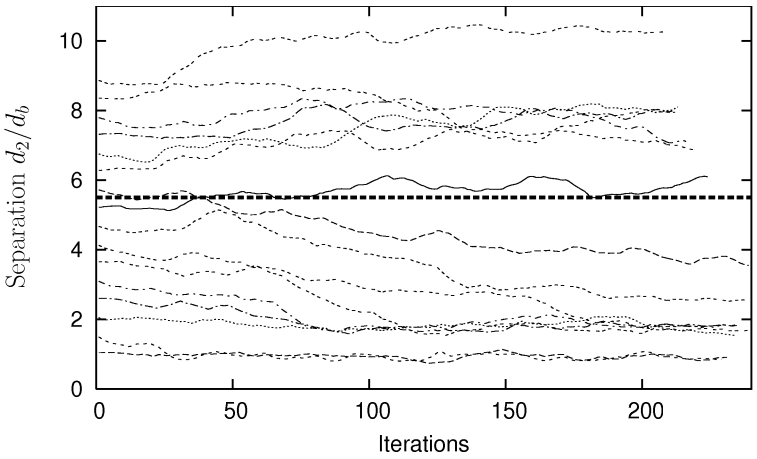

Fig. 9. The separation, measured in bubble diameters, between two discs falling through a foam in configuration 2 with $N = 1500$ bubbles. It can be seen that for discs initially separated by up to $2d_b$, the discs descend in the foam at a constant separation. If the discs are initially separated by 2 to $5d_b$, then they move closer together until they eventually reach a separation of 1 to $2d_b$, after which the motion is stable. If the initial separation is greater than about $5d_b$ then the variation in separation is less and they stay far apart. Here the yielded region above the lower disc (the wake) plays an important role in the interaction of the discs.

3.3 Two discs falling in configuration 2

We consider two discs descending in the foam, starting one above the other. We vary the initial separation between two discs of area $A_d = 4A_b$ to interpret how the discs interact when they are oriented in this way (figure 5(b)).

3.3.1 Disc Position

Discs that start one above the other remain in this orientation as they descend through the foam. The wake of the lower disc is represented by the yielded region of the foam and it is this that determines how the discs interact. Discs that start sufficiently close move together until they are separated by only one or two bubbles, after which they move at a constant separation. This is illustrated in figure 9, where it is apparent that the critical separation is now greater than for configuration 1; for discs of area $A_d = 4A_b$ the critical separation is $d_2^c \approx 5d_b$.

3.3.2 Forces on the discs

The role that the drag force plays in this interaction pattern is described in figure 10. The lift force is assumed to be negligible as the discs are placed at the centre of the foam channel. To clarify the effect that varying the initial

separation has on the drag force differences on both discs, figure 10 needs to be split into three regions where the interaction between the discs differs. For initially close discs ($d_2^{\text{init}} < 2d_b$) the drag force difference between the discs is negligible, whence they will move through the foam at constant separation. However, when the discs are initially separated by a larger distance, $2d_b < d_2^{\text{init}} < 5d_b$, the difference between the drag forces on the discs increases. The drag on the lower disc is always greater than that on the upper disc so they will move closer together as the upper disc moves into the other disc's wake. When the discs are even further apart (more than $5d_b$ separation) the drag force differences become less in magnitude. In some cases there is a greater drag force on the upper disc, but in general there is limited interaction between the two discs.

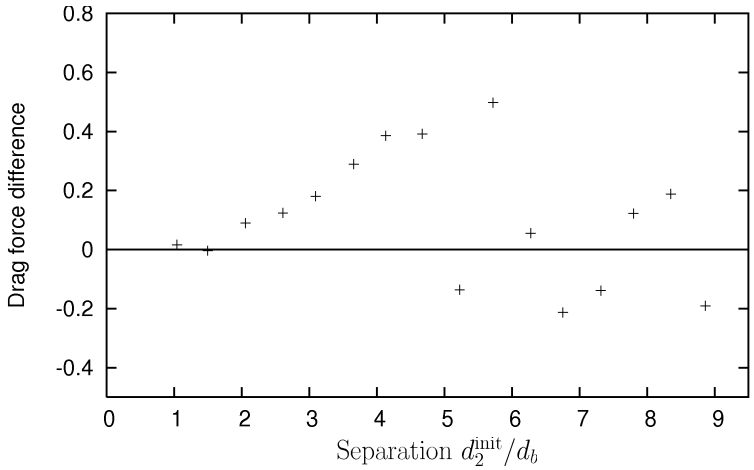

Fig. 10. Variation of the difference in average drag force of both discs falling in configuration 2 as the initial separation between them is varied. The difference in drag is measured by subtracting the drag force on the upper disc from the drag force on the lower disc. We see that when the discs are close together ($0 < {d_2}^{\text{init}}/d_b < 2$), the difference between the drag force is close to zero. For increasing initial separations ($2 < {d_2}^{\text{init}}/d_b < 5$), the differences in drag force between the discs increases; here, the drag on the lower disc is greater than that of the upper disc, so that the upper disc descends more quickly than the lower disc and moves into its wake. Increasing the initial separation further (${d_2}^{\text{init}}/d_b > 6$) leads to the differences in the drag force on both discs becoming scattered in a random manner, and the discs therefore don't interact.

4 Conclusions

The interaction between a sedimenting disc and a wall is small, although a small attractive force exists when the disc is in close proximity to the wall. Thus for our simulations of two sedimenting discs, we worked far enough away from the wall so that we could neglect these effects.

In the case of two discs sedimenting initially side-by-side, a rotation towards a configuration in which they are one above the other is evident. The rate of rotation is dependent on the initial separation between the discs and the size of the discs. For discs of size $A_d = 4A_b$, this interaction only occurs if the initial separation between the discs is less than 3 to 4 bubble diameters. When the initial separation is greater than 4 bubble diameters the foam screens the interaction and the motion of each disc is determined by variations in the local structure of the foam. This critical separation increases with disc size.

For the case in which one disc sediments above another, further evidence of screening is apparent. The initial separation of the discs is again an important parameter that determined their interaction. If the discs are placed a little way apart (between 2 and $5d_b$ for the disc areas considered here) then they move closer together due to the drag force on the lower disc being greater than that of the upper disc. In this case the upper disc is sedimenting in the yielded region of the foam behind the lower disc. Once the discs reach a separation of $1 - 2d_b$, the drag force on both is equal and they therefore move at the same rate. However, if the initial separation is large then the drag force on each disc is independent and they don't interact.

Thus the motion of the discs is stable when their line of centres is parallel to the direction of gravity and separated by one to two bubbles. Although this is reminiscent of elastic fluids, the plasticity of the foam plays an important rôle: the T_1 events behind the discs as bubbles lose contact change the local structure of the foam and allow the upper disc in the wake to move more quickly. The discrete nature of the foam means that objects don't interact if they are separated by more than a certain number of bubbles either horizontally or vertically.

It remains to be seen whether these results extend to objects of different dimensions, (weight) or shape (e.g. ellipses), and to what extent material parameters such as the bubble area dispersity and the liquid fraction of the foam dictate the dynamics of sedimentation. Boundary conditions on the channel walls and disc edges, for example a relaxation of the no-slip condition on the wall, may change the details of the rotatory motion, but will not suppress it.

Inclusion of the viscous forces on the discs may lead to increased rotation of the discs, and simulations that implement this are likely to provide a better comparison with experiment.

References

[1] D. Weaire and S. Hutzler. *The Physics of Foams.* Oxford University Press, 2000.

[2] R. K. Prud'homme and S.A. Khan, editors. *Foams: Theory, Measurements and Applications.* CRC Press, 1996.

[3] J. J. Bikerman. *Foams: Theory and Industrial Applications.* Reinhold Publishing Corporation, New York, 1953.

[4] R. Hhler and S. Cohen-Addad. Topical review - rheology of liquid foam. *J. Physics: Condensed Matter*, 17:R1041–R1069, 2005.

[5] G. G. Stokes. On the effect of the inertial friction of fluids on the motion of pendulums. *Trans. Camb. Phil. Soc.*, IX:8–149, 1850.

[6] S. J. Cox, M. D. Alonso, S. Hutzler, and D. Weaire. The Stokes Experiment in a Foam. In P. Zitha, J. Banhart and G. Verbist, editor, *Foams, Emulsions and their Applications*, pages 282–289. MIT-Verlag, Bremen, 2000.

[7] I. Cantat and O. Pitois. Stokes experiment in a liquid foam. *Phys. Fluids*, 18, 2006.

[8] J.R. de Bruyn. Transient and steady-state drag in a foam. *Rheol. Acta.*, 44: 150–159, 2004.

[9] J.R. de Bruyn. Age dependence of the drag force in an aqueous foam. *Rheol. Acta*, 45:801–811, 2005.

[10] I. Cantat and O. Pitois. Mechanical probing of liquid foam ageing. *J. Phys. Condens. Matter*, 17:S3455–S3461, 2005.

[11] S. J. Neethling and J. J. Cilliers. Solids motion in flowing froths. *Chemical Engineering Science*, 57:607–615, 2002.

[12] H.T. Lee, S.J. Neethling, and J.J. Cilliers. Particle and liquid dispersion in foams. *Colloids Surf. A*, 263:320–329, 2005.

[13] B. Dollet, F. Elias, C. Quilliet, A. Huillier, M. Aubony, and F. Graner. Two-dimensional flows of foam: drag exerted on circular obstacles and dissipation. *Colloids Surf. A*, 263:101–110, 2005a.

[14] B. Dollet, F. Elias, C. Quillet, C. Raufaste, M. Aubony, and F. Graner. Two-dimensional flow of foam around an obstacle: Force measurements. *Phys. Rev. E*, 71:031403, 2005b.

[15] B. Dollet and F. Graner. Two-dimensional flow of foam around a circular obstacle: local measurements of elasticity, plasticity and flow. *J. Fluid Mech.*, 585:181–211, 2007.

[16] C. Raufaste, B. Dollet, S. Cox, Y. Jiang, and F. Graner. Yield drag in a two-dimensional foam flow around a circular obstacle: Effect of liquid fraction. *Euro. Phys. J. E.*, 23:217–228, 2007.

[17] B. Dollet, M. Aubouy, and F. Graner. Anti-inertial lift in foams: A signature of the elasticity of complex fluids. *Phys. Rev. Lett.*, 95, 2005c.

[18] B. Dollet, M. Durth, and F. Graner. Flow of foam past an elliptical obstacle. *Phys. Rev. E*, 73, 2006.

[19] J. Wang and D. D. Joseph. Potential flow of a second-order fluid over a sphere or an ellipse. *J. Fluid Mech.*, 511:201–215, 2004.

[20] S.J. Cox, F. Graner, and M.F. Vaz. Screening in two-dimensional foams. *Soft Matter*, 4:1871–1878, 2008.

[21] K. Brakke. The Surface Evolver. *Exp. Math.*, 1:141–152, 1992.

[22] S. Daugan, L. Talini, B. Herzhaft, and C. Allain. Aggregation of particles settling in shear-thinning fluids. *Eur. Phys. J. E*, 7:73-81, 2002.

[23] B. Gueslin, L. Talini, B. Herzhaft, Y. Peysson, and C. Allain. Aggregation behaviour of two spheres falling through an aging fluid. *Phys. Rev. E 74*, 74, 2006.

[24] J. Feng, P. Y. Huang, and D. D. Joseph. Dynamic simulation of sedimentation of solid particles in an Oldroyd-b fluid. *J. Non-Newtonian Fluid Mech.*, 63: 63–88, 1996.

[25] D. D. Joseph, J. Y. Liu, M. Poletto, and J. Feng. Aggregation and dispersion of spheres falling in viscoelastic liquids. *J. Non-Newtonian Fluid Mech.*, 54:45–86, 1994.

[26] A. Wyn, I. T. Davies, and S. J. Cox. Simulations of two-dimensional foam rheology: Localization in linear Couette flow and the interaction of settling discs. *Eur. Phys. J. E*, 26:81–89, 2008.

[27] S.J. Cox, B. Dollet, and F. Graner. Foam flow around an obstacle: simulations of obstacle-wall interaction. *Rheol. Acta.*, 45:403–410, 2006.

[28] D. D. Joseph and J. Feng. A note on the forces that move particles in a second-order fluid. *J. Non-Newtonian Fluid Mech.*, 64:299–302, 1996.

[29] K. Brakke. 200,000,000 Random Voronoi Polygons. *www.susqu.edu/brakke/papers/voronoi.htm*, 1986, unpublished.